

## Photodissociation of a Surface-Active Species at a Liquid Surface: A Study by Time-of-Flight Spectroscopy

Alan Furlan<sup>†</sup>

Physikalisch-Chemisches Institut der Universität Zürich, Winterthurerstrasse 190, CH-8057 Zürich, Switzerland

Received: October 13, 1998; In Final Form: January 8, 1999

The photochemistry at a gas–liquid interface was investigated by time-of-flight/quadrupole mass spectroscopy (TOF/QMS). A thin liquid film of 4-iodobenzoic acid (IBA), dissolved in glycerol, was irradiated with nanosecond laser pulses at 275 nm. Atomic and molecular iodine were the only photoproducts leaving the liquid after a low-fluence laser pulse ( $<5 \text{ mJ/cm}^2$ ). The amount of released I atoms was 2 orders of magnitude larger than the amount of desorbed  $\text{I}_2$ . Model calculations were carried out that take into account laser photolysis of IBA, diffusion, and surface evaporation of I and  $\text{I}_2$ , and the condensed-phase kinetics of radical reactions. Ejection of hyperthermal I atoms by direct photodissociation of surface layer molecules is also considered. The quantitative analysis is restricted to low laser fluence conditions at which laser-induced heating of the illuminated liquid is negligible. The results of the model calculations were compared to previously obtained TOF data of an alkyl iodide ( $\text{C}_{18}\text{H}_{37}\text{I}$ ) dissolved in the apolar liquid squalane ( $\text{C}_{30}\text{H}_{62}$ ). The velocity distribution of the iodine atoms from the alkyl iodide solution corresponds to the temperature of the liquid (278 K). The contribution of I atoms from depths greater than 1 nm is large ( $>99\%$ ). In contrast, I atoms desorbing from IBA/glycerol are hyperthermal ( $T_{\text{trans}} = 480 \text{ K}$ ) and originate almost exclusively from the topmost molecular layer (1 nm). TOF measurements with a fast chopper wheel in front of the surface provide the time-dependent desorption flux from the surface and confirm that the contribution from deeper layers in the alkyl iodide solution is much larger than in the aryl iodide solution. Model calculations predict the behavior of the two solutions correctly if differences in caging of the geminate pair, diffusion coefficients of the free radicals, and the set of bulk radical reactions in the two solutions are taken into account. The hyperthermal energies of the ejected I atoms from the IBA solution are discussed in terms of the surface orientation of excited IBA molecules. The dependence of the TOF spectra on laser power and IBA concentration is interpreted by a surface excess of IBA. The result is compared to temperature-dependent surface tension measurements of IBA solutions in glycerol and water. The response of the surface tension to an accumulation of IBA at the surface is very weak.

### 1. Introduction

The photochemistry at gas–liquid interfaces is of great theoretical and practical interest, in particular since it has been realized that processes occurring on atmospheric cloud particles and aerosols have a large impact on photochemical cycles responsible for the destruction of ozone.<sup>1–3</sup> Applications of photochemistry at gas–liquid interfaces can be found in various fields including photography, bleaching, analytical methods such as matrix-assisted laser desorption and ionization, and photo-induced reactions on biological tissues exposed to UV radiation.<sup>4</sup> The fate of a molecule in the liquid that is excited to a repulsive electronic state depends on the location and orientation of the species with respect to the interface. If the excited species is located in the topmost liquid layer, the bond cleavage may be followed by direct ejection of the fragments into the gas phase. If the axis of the breaking bond is oriented parallel to the surface, the recoiling fragments will collide with surrounding molecules and desorb with a reduced kinetic energy. Fragments originating from chromophores in deeper layers of the liquid will mostly recombine geminately because of the surrounding solvent cage, and the energy will be dissipated as heat.

Compared to gas–solid interfaces, it has been difficult to obtain structural and orientational information about molecules

at liquid–gas interfaces, in part because of the technical problems in studying clean liquid surfaces under clean, high-vacuum conditions. Only in the past decade have new techniques been developed, including sum-frequency mixing<sup>5</sup> and molecular beam surface scattering,<sup>6</sup> which reveal molecular details of gas–liquid interfaces such as surface coverage and orientation of surface molecules in liquid mixtures.<sup>7–9</sup> Another technique often used to analyze photodissociation processes at *solid* surfaces is the time-of-flight method combined with quadrupole mass spectroscopy (TOF/QMS).<sup>10</sup> Owing to the universal detection method (ionization by electron bombardment), virtually any photoproduct can be identified. In addition, a TOF spectrum of the desorbed products reveals the history of the species between the laser pulse and the time of desorption and thus indirectly probes the structure and orientation of the surface. In our laboratory the TOF/QMS method has been recently applied for the first time to the study of photoproducts ejected from *liquid* surfaces.<sup>11,12</sup> The liquid film preparation technique developed by Fenn et al.<sup>13</sup> and Nathanson et al.<sup>6</sup> was used for producing clean, renewed liquid surfaces of long-chain alkyl iodides (1-iodododecane<sup>11</sup> and 1-iodooctadecane in squalane<sup>12</sup>) in high vacuum. At high enough laser fluences ( $>10 \text{ mJ/cm}^2$ ) the photoexcitation pulse was found to be followed by explosive desorption of the ejected species. At fluences less than  $5 \text{ mJ/cm}^2$ , the velocities of the photoproducts, atomic I, HI, and  $\text{I}_2$ ,

<sup>†</sup> E-mail: furlan@pci.unizh.ch.

were in full thermal equilibrium with the surrounding liquid. The time-dependent desorption flux of these species was obtained by using a fast chopper wheel in front of the surface synchronized with the laser pulse. By comparison of the TOF spectra with numerical simulations, it was demonstrated that a considerable fraction of the ejected photoproducts originate from deeper layers within the liquid. The absence of prompt hyperthermal I fragments was interpreted as a preferential orientation of the alkyl iodide molecules in the topmost layer with the I atom pointing into the liquid.

This study is a continuation of our previous work<sup>11,12</sup> with amphiphilic molecules. These molecules tend to accumulate at the surface of a polar solvent. As a test system, 4-iodobenzoic acid (IBA) was chosen as a chromophore, dissolved in glycerol. The photodissociation mechanism of isolated IBA molecules is expected to be similar to the mechanism of related compounds such as iodobenzene and other aryl halides.<sup>14</sup> In contrast to alkyl iodides, the cleavage of the C–I bond in aryl iodides is an indirect process.<sup>14</sup> Excitation in the range  $250 \pm 30$  nm promotes the molecules to the  $(\pi, \pi^*)$  state. After internal conversion to the repulsive  $(n, \sigma^*)$  state on a time scale of 0.5–1.0 ps, the C–I bond breaks promptly.<sup>14–16</sup> A fraction of 30–50% of the excess energy is partitioned to translational recoil of the fragments.<sup>15</sup>

In our previous study of alkyl iodide dissolved in squalane an estimate of the surface sensitivity was obtained based on model calculations. For that system it was found that hyperthermal photofragments from the topmost liquid layer should be detected if their fraction exceeded 1–10% of all photofragments formed in the surface layer.<sup>12</sup> A goal of this study is to test this prediction with a system for which ejection of hyperthermal fragments from the surface is expected. Since IBA is an amphiphilic molecule, it may accumulate at the surface. The surface orientation of IBA is unknown. However, it can be speculated that the –COOH group points preferentially into the bulk liquid and forms H-bonds with the polar solvent, whereas the –I end is preferentially directed out of the liquid. If this preferential orientation of IBA at the surface is correct, one would expect that the fastest I fragments desorb without collisions and exhibit a velocity distribution similar to that of gas-phase photodissociation.<sup>17,18</sup> Another aim of this work is to determine the relative yield of hyperthermal fragments, which represents a measure of the surface accumulation of the chromophore. The partitioning of the chromophore between bulk and surface as obtained from the TOF spectra will be compared to surface tension measurements and to our previous measurements with alkyl iodide.

## 2. Experimental Section

The technique used to prepare clean and continuously renewed liquid surfaces in a vacuum has been described elsewhere.<sup>6,12</sup> Briefly, a rotating aluminum wheel is submerged in a reservoir filled with the liquid. The high viscosity of the liquid studied here required a low rotation speed of 0.2 Hz. To improve the wetting of the wheel, the surface was roughened and patterned with spiraling grooves. No scraper was used to allow for molecular ordering of the surface layer of the liquid. Solutions of the photoabsorbing species 4-iodobenzoic acid (>98%, Fluka) in glycerol (>99.5%, Fluka) were prepared at concentrations of  $4 \times 10^{-5}$  and  $2 \times 10^{-6}$  mol/L. The concentrations were determined spectrophotometrically. The extinction coefficient  $\epsilon$  of IBA in methanol is  $1.7 \times 10^4$  dm<sup>3</sup> mol<sup>-1</sup> cm<sup>-1</sup> at the peak of the absorption band at 250 nm and is  $4 \times 10^3$  dm<sup>3</sup> mol<sup>-1</sup> cm<sup>-1</sup> at 275 nm, the excitation wavelength

used in this study. The liquid was cooled to 5 °C by Peltier elements attached to the bottom of the reservoir and controlled with a thermocouple. The pressure in the source chamber surrounding the liquid container was about  $5 \times 10^{-6}$  mbar. The insertion of a liquid-nitrogen-cooled trap with a coldfinger in front of the liquid reservoir reduced the pressure to  $\leq 1 \times 10^{-6}$  mbar but had no effect on the TOF spectra.

Excitation laser pulses at 275 nm and pulse energies of 25  $\mu$ J to 12 mJ/pulse ( $\tau \approx 6$  ns and  $\Delta\nu \approx 0.15$  cm<sup>-1</sup>) were obtained by frequency-doubling the output of a Nd:YAG-pumped dye laser.

The collimated laser beam was focused horizontally with a 700 mm cylindrical lens and directed onto the liquid surface at a grazing angle of 87°. The illuminated liquid surface area was determined to be  $2 \times 6$  mm<sup>2</sup> by measuring the spot area at normal incidence with a CCD camera and considering the expansion in one direction due to the grazing incidence angle. The reflection loss of the s-polarized laser beam impinging at 87° is 82%. The resulting laser fluence of the beam refracted into the liquid is in the range 0.05–20 mJ/cm<sup>2</sup>. The penetration depth within which the intensity falls to 1/e is 60 nm for a  $4 \times 10^{-5}$  mol/L solution, much larger than the film thickness. The reflected light was directed out of the chamber via a dichroic mirror.

The detector is contained in a bakeable ultrahigh vacuum system consisting of three differentially pumped stages.<sup>19</sup> After a total flight distance of 374 mm the molecules were ionized by impact with 130 eV electrons and mass-filtered in a QMS. A time offset of 3.9  $\mu$ s ( $(m/e)^{1/2}$ ) was subtracted from the measured TOF spectra in order to correct for the transit time of the ions through the mass filter.<sup>19</sup> Some of the TOF measurements were carried out with a chopper wheel inserted at a distance of 34 mm from the surface. The wheel (80 mm diameter, one 0.7 mm slit) spins at 200 Hz and is synchronized with the laser, producing an open duration of about 15  $\mu$ s at selectable times following the laser-surface interaction.

The accumulation of surface contaminations during the measurements was checked by measuring the surface tension with a De Nouy ring attached to an electronic balance (Sigma 703).<sup>20</sup> Unchanged values before and after measurements indicated that the surface remained clean during the measurement time. Temperature-dependent measurements of the surface tension were carried out with a Wilhelmy plate.<sup>20</sup> Peltier elements attached to the liquid reservoir allowed the temperature to be varied in the range 0–100 °C. The tensiometer was enclosed in a box purged with nitrogen to avoid contamination of the liquid by water vapor and greasy particles. The temperature was changed in steps of 10 K and left to equilibrate for 20 min. No hysteresis of the surface tension was observed between warming and cooling phases. The values obtained in several cycles were constant within  $\pm 0.2$  mN/m.

## 3. Results

**TOF Spectra.** Following irradiation of the IBA/glycerol film with low-fluence pulses ( $\leq 5$  mJ/cm<sup>2</sup>) at 275 nm, a signal was observed exclusively at the mass of atomic iodine,  $m/e = 127$ , and molecular iodine,  $m/e = 254$ .<sup>21</sup> The TOF spectrum recorded at  $m/e = 127$  is shown in Figure 1a for an IBA concentration of  $4 \times 10^{-5}$  mol/L. The TOF signal of I<sub>2</sub><sup>+</sup> (not shown) was weaker than the I<sup>+</sup> signal by a factor of 80 (corrected for ionization efficiencies and I<sub>2</sub> cracking<sup>12</sup>). Only about 1% of the observed  $m/e = 127$  signal originates in cracking of I<sub>2</sub>, as determined in a separate experiment with a pure I<sub>2</sub> source. The shape of the I<sub>2</sub><sup>+</sup> profile is similar to the I<sub>2</sub><sup>+</sup> spectrum as displayed

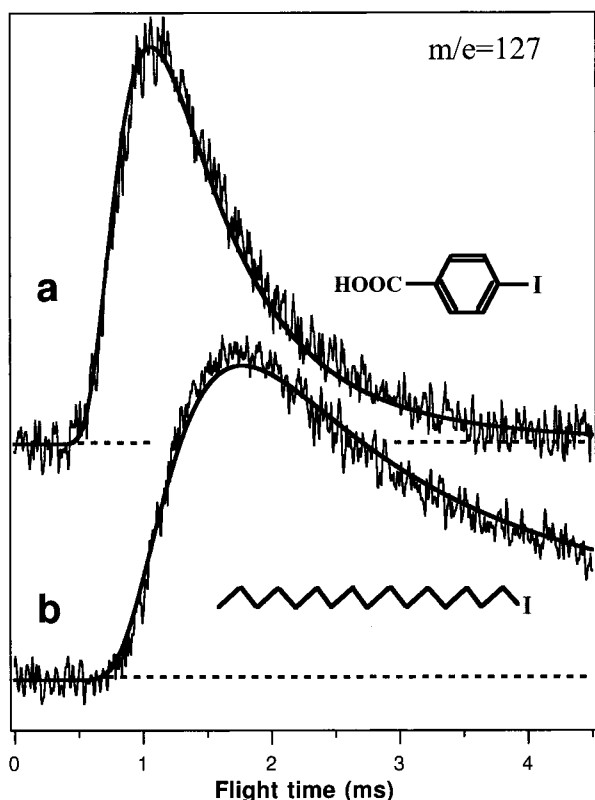


**Figure 1.** TOF distributions of iodine atoms ( $m/e = 127$ ) following irradiation of liquids with iodine-containing chromophores at 275 nm and a laser fluence of  $0.6 \text{ mJ/cm}^2$ . The chromophore in spectrum a was 4-iodobenzoic acid ( $4 \times 10^{-5} \text{ mol/L}$ ) dissolved in glycerol. Spectrum b was obtained by irradiation of a  $0.1 \text{ M}$  1-iodooctadecane ( $\text{C}_{18}\text{H}_{37}\text{I}$ ) solution in squalane ( $\text{C}_{30}\text{H}_{62}$ ). The model simulations of the spectra, shown as solid lines, are described in the text.

in Figure 2 of ref 12, with a late onset at about 1.5 ms and a slow decay. However, the  $\text{I}_2^+$  signal was too weak to allow measurements with a chopper wheel. The  $\text{I}_2$  profiles could therefore not be used for the quantitative analysis that is presented in the next section. No signal was found at the masses of the parent molecule IBA,  $m/e = 248$ , the benzoic acid fragment,  $m/e = 121$ , or HI,  $m/e = 128$ . The limited resolution of the QMS in the mass range  $>100 \text{ amu}$  ( $\text{fwhm} \approx 2 \text{ amu}$ ) required a calibration measurement to distinguish between I and HI.<sup>12</sup> From the complete overlap of the nominal  $m/e = 127$  peak observed in a pure  $\text{I}_2$  beam with the  $m/e = 127$  peak produced with the irradiated liquid, it was concluded that no HI is ejected off the irradiated liquid.

In Figure 1b the TOF profile of I atoms desorbed from a  $0.1 \text{ M}$  1-iodooctadecane ( $\text{C}_{18}\text{H}_{37}\text{I}$ ) solution in squalane ( $\text{C}_{30}\text{H}_{62}$ ) is shown. This TOF profile has a later onset and a slower decay at long flight times compared to the spectrum of the IBA/glycerol solution (Figure 1a). Both spectra shown in Figure 1 were recorded at a low laser fluence of  $0.6 \text{ mJ/cm}^2$ . The goal of the TOF measurements presented in the following is to explore the different shapes of profiles in spectra a and b of Figure 1. In general, the signal decay at long flight times is a signature of species originating from deeper liquid layers. The late arrival time at the detector is due to diffusion of these photoproducts to the surface followed by delayed desorption. On the other hand, the difference in signal onsets reflects a different degree of thermalization of the nascent fragments before they leave the surface. If the desorbing species exhibit a highly hyperthermal velocity distribution similar to gas-phase photofragments, the orientation of the excited molecule in the

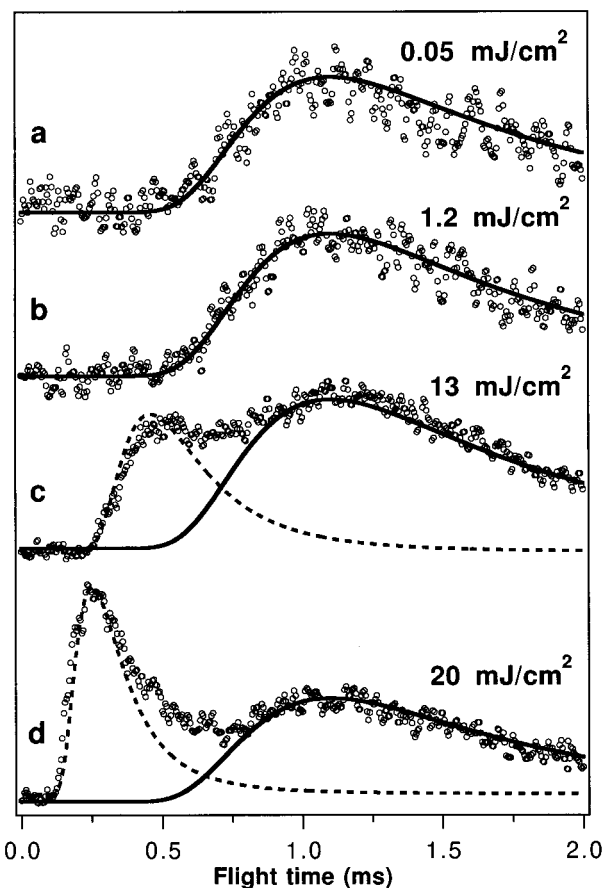


**Figure 2.** TOF distributions of I atoms ( $m/e = 127$ ) recorded at laser fluences between  $0.05$  and  $20 \text{ mJ/cm}^2$ . The relative scaling of the spectra is arbitrary, since acquisition times were adjusted depending on the signal level. The solid lines represent Maxwell-Boltzmann distributions with a temperature of  $T_{\text{trans}} = 480 \text{ K}$ . The dotted lines in curves c and d are shifted Maxwell-Boltzmann distributions with  $T_{\text{trans}} = 1300$  and  $2500 \text{ K}$  and stream velocities  $v_s = 500$  and  $1000 \text{ m/s}$ , respectively.

surface layer must have allowed collision-free or nearly collision-free desorption. The signal onset also strongly depends on laser fluence. A series of TOF spectra of IBA in glycerol at different laser fluences are shown in Figure 2. In the range  $0.05$ – $5 \text{ mJ/cm}^2$  the shape of the TOF profiles is unchanged (curves a and b of Figure 2), indicating that at these low fluences laser-induced heating of the illuminated liquid is negligible. However, the TOF distributions change substantially at laser fluences above approximately  $10 \text{ mJ/cm}^2$  and become bimodal (curves c and d of Figure 2). A fast component grows quickly and shifts toward shorter flight times with increasing laser fluence. This fast part can be modeled by a stream velocity  $v_s$  superimposed on a Maxwell-Boltzmann distribution. This type of distribution is often found in ablation studies when the desorption flux is large enough to allow gas-phase collisions.<sup>22,23</sup> The collisions lead to a fast particle beam directed perpendicular and away from the surface. At the low fluences ( $<5 \text{ mJ/cm}^2$ ) discussed in the following, however, gas-phase collisions have a low probability.<sup>11</sup>

From a comparison of the onset of ablative desorption occurring at  $\sim 10 \text{ mJ/cm}^2$  with the theoretically expected onset, which will be discussed in the next section, it appears that IBA tends to accumulate at the gas-liquid interface. To test this hypothesis, a series of dilution measurements was performed. As shown in Figure 3, a dilution of the IBA solution by a factor of 20 does not affect the shape of the TOF profiles, and the signal intensity is only reduced by a factor of 2–3. If the surface

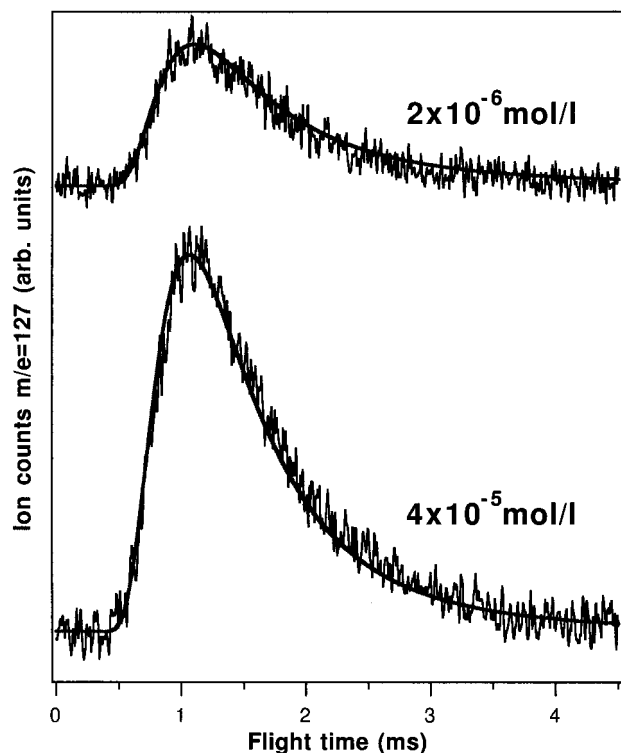


**Figure 3.** TOF spectra of iodine atoms ejected from IBA/glycerol solutions at two different IBA concentrations: (a)  $4 \times 10^{-5}$  mol/L; (b)  $2 \times 10^{-6}$  mol/L. Both spectra were recorded at a laser fluence of 0.6 mJ/cm<sup>2</sup>.

concentration of IBA were equal to the bulk concentration, a reduction proportional to the dilution factor would be expected. No signal reduction should occur if the topmost liquid layers consisted of pure IBA. The small signal reduction observed in our measurements clearly confirms an accumulation of IBA at the liquid surface.

As noted above, Figure 1 reveals, apart from a later onset, also a much slower decay of the I signal in the C<sub>18</sub>H<sub>37</sub>I/C<sub>30</sub>H<sub>62</sub> system (Figure 1b) compared to that in IBA/glycerol (Figure 1a). The slow decay is a consequence of I atoms originating from deeper liquid layers and desorbing at long delay times after the laser pulse. A detailed discussion of delayed desorption in the system C<sub>18</sub>H<sub>37</sub>I/C<sub>30</sub>H<sub>62</sub> is given in ref 12. The fast decay of the I signal in the IBA/glycerol spectrum (Figure 1a) suggests that the desorption flux at long delay times is comparatively small. This result is confirmed by a series of measurements with a chopper wheel synchronized to the laser pulses. Chopped spectra of I atoms from IBA are shown in Figure 4 for three different laser-chopper delays. As described in ref 12 late desorption of species can be distinguished by a broad shoulder in the chopped profiles at short flight times. This feature is completely absent in the profiles displayed in Figure 4a, confirming that desorbing I atoms originate almost exclusively from depths less than 1 nm from the liquid–gas interface, which corresponds approximately to the topmost molecular layer. The best-fit simulations of the chopped TOF profiles are shown in parts b and c of Figure 4 for IBA/glycerol and C<sub>18</sub>H<sub>37</sub>I/C<sub>30</sub>H<sub>62</sub>, respectively. The shapes exhibit considerable differences for the two systems. The chopped profiles in Figure 4b consist of a single peak at all delay times. In contrast, the simulations in Figure 4c exhibit a shoulder at short flight times, which grows to a second peak at large laser-chopper delays. This second feature indicates a signal contribution from depths greater than 1 nm, which is much larger in C<sub>18</sub>H<sub>37</sub>I/C<sub>30</sub>H<sub>62</sub> because of the

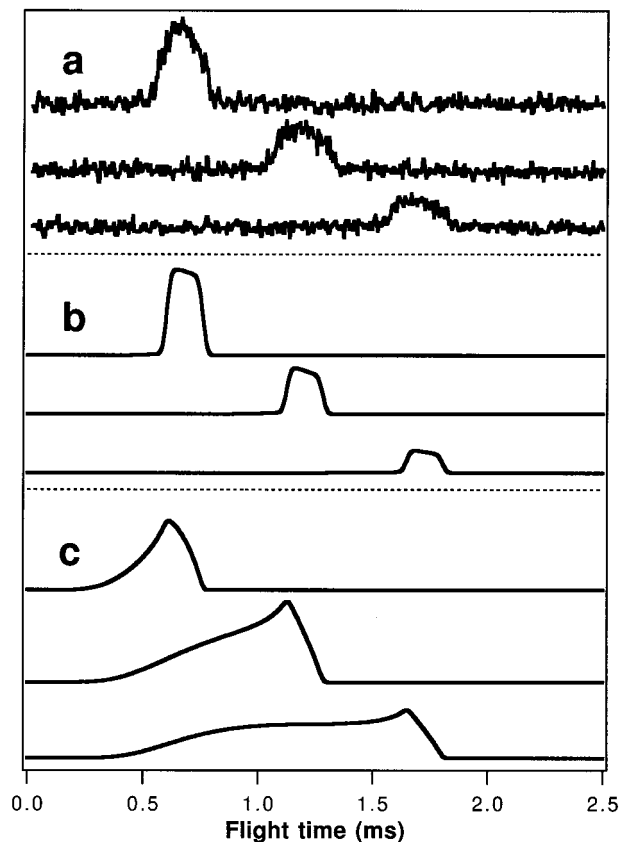


**Figure 4.** (a) Chopped TOF spectra at  $m/e = 127$  of IBA/glycerol recorded at three different delays between the laser shot and the chopper opening (100, 150, and 200  $\mu$ s). (b) Simulations of the chopped IBA/glycerol spectra with  $T_s = 480$  K. (c) Best-fit simulations of the chopped iodoctadecane/squalane spectra with  $T_s = 298$  K. The chopped profiles of IBA/glycerol are dominated by desorption of incompletely thermalized I atoms from the topmost liquid layer, whereas the iodoctadecane/squalane system exhibits a larger contribution from late desorption, evident as a broad shoulder at short flight times of the chopped profiles.

larger cage escape probability and smaller viscosity of squalane. It must be noted that the TOF spectra of iodoctadecane/squalane recorded at  $m/e = 127$  contain a contribution from HI molecules, which is not present in the IBA/glycerol system. However, the I and HI profiles are very similar in shape. A detailed discussion of the shapes of chopped profiles was given in ref 12.

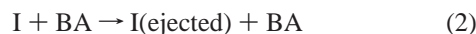
**Surface Tension Measurements.** Surface tension measurements are often used to probe the accumulation of surface-active species at the liquid surfaces. The surface tension of IBA in glycerol was determined at different IBA concentrations between  $1 \times 10^{-6}$  and  $1.3 \times 10^{-4}$  mol/L. The upper value corresponds to a saturated solution at 25 °C. A constant value  $\sigma = 62.0 \pm 0.2$  mN/m, equal to the surface tension of pure glycerol, was obtained in the whole concentration range. The temperature dependence of the surface tension, shown in Figure 5, was determined between 5 and 95 °C for  $4 \times 10^{-5}$  mol/L IBA solutions in glycerol and water. The values obtained for the pure solvents are displayed by full dots. Within the experimental error bounds of  $\pm 0.2$  mN/m no difference was observed between the IBA/glycerol solution and pure glycerol. The precision of the measurements is mainly limited by changes in wetting of the Wilhelmy plate over longer measurement periods. The surface tension of the aqueous IBA solution was found to be on average  $1.0 \pm 0.2$  mN/m lower than that of pure water, with the difference decreasing from 1.7 mN/m at 5 K to 0.6 mN/m at 90 K.

#### 4. Quantitative Analysis of TOF Spectra

The model calculations used to analyze the TOF spectra have been described in detail elsewhere.<sup>12</sup> Briefly, the time-dependent concentration profiles of I and I<sub>2</sub> are computed by numerical integration of one-dimensional coupled differential equations, which govern the diffusion and surface evaporation of both species, and the kinetics of radical combination. Absorption of laser light by IBA molecules is followed by dissociation of the excited species and production of benzoic acid radicals and iodine radicals at the surface and within the liquid.



I fragments formed at the surface can be directly ejected into the gas phase:



The desorption energy of the benzoic acid radical BA is relatively large owing to hydrogen bonding to glycerol molecules. The desorption rate of BA at 278 K is therefore expected to be very low, in agreement with experimental results, and is neglected in the calculation.

Radicals formed in deeper layers of the liquid are surrounded by a cage of glycerol molecules. These radicals will recombine geminately (reaction 3), or escape from the cage (reaction 4).



The braces indicate the liquid cage surrounding the geminate pair. The mobile radicals (reaction 4) diffuse freely in solution and undergo combination reactions 5–7.



The radical reactions 5–7 are exothermic, have no activation barrier, and are modeled with diffusion-limited rates approximated by the form  $k \approx 8RT/(3\eta)$  dm<sup>3</sup> mol<sup>-1</sup> s<sup>-1</sup>.<sup>24</sup> All steric factors were arbitrarily neglected for the sake of simplicity. The reaction scheme previously used to model the bulk photochemistry of C<sub>18</sub>H<sub>37</sub>I in squalane was equivalent to reactions 1–7 presented above but included a few more reactions that can be neglected in IBA/glycerol.<sup>12</sup> Most importantly, the formation of HI according to



does not occur with the reaction pair {I + BA}. In contrast to the exothermic  $\alpha$ -H abstraction of reaction 8, the  $\beta$ -H abstraction from BA is endothermic. The simulation only considers diffusion of I and I<sub>2</sub> in the direction perpendicular to the surface, since the illuminated surface area (2 × 6 mm<sup>2</sup>) is much larger than the liquid depth relevant in the TOF experiment. The I and I<sub>2</sub> desorption flux from depths greater than or equal to 1  $\mu$ m is negligible, since the large viscosity of glycerol (~5000 cP at 5 °C) prevents larger diffusion lengths on the millisecond time scale of the experiment. The diffusion constants of I and I<sub>2</sub> are estimated to be 1 × 10<sup>-12</sup> and 2 × 10<sup>-13</sup> m<sup>2</sup>/s, respectively, on the basis of scaling of published values for I<sub>2</sub> in hexane with viscosity of the solvent and on hydrodynamic radii and mass factors of the solute.<sup>24</sup> Within a 1  $\mu$ s time step

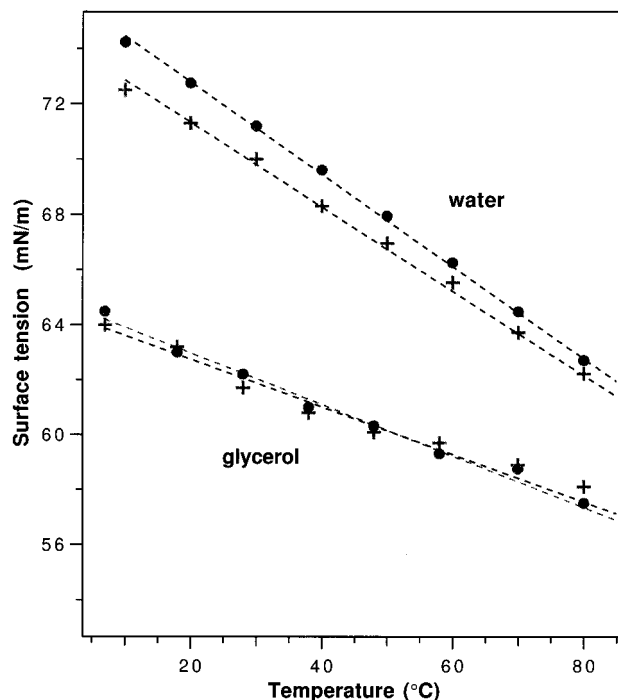


**Figure 5.** Surface tensions of a  $4 \times 10^{-5}$  mol/L solution of 4-iodobenzoic acid in glycerol and in water as a function of temperature (crosses). The surface tensions of pure glycerol and water are also shown (full dots). The size of the markers indicates the error bounds.

of the numerical calculation, the mean diffusion length of I<sub>2</sub> in glycerol is  $(2Dt)^{1/2} \approx 0.7$  nm, 14 times smaller than the mean diffusion length of I<sub>2</sub> in squalane.

The initial depth-dependent concentrations of benzoic acid and iodine radicals are calculated from the laser fluence, the optical density of the sample, and the escape probability for avoiding geminate recombination  $k_4/(k_3 + k_4)$ . The evaporative escape of I and I<sub>2</sub> is simulated with a rate proportional to the concentration in the surface layer and the respective diffusion constant. The time-dependent flux of I and I<sub>2</sub> leaving the surface is used to calculate the total TOF signals and the TOF signals through the chopper wheel, assuming thermal velocity distributions. A contribution of prompt, hyperthermal I atoms from a surface layer (reaction 2) can be modeled for a given translational energy distribution.

In Figure 6 the TOF spectrum of iodine atoms is shown together with various model simulations. In this simple calculation the liquid is subdivided into a surface layer of variable thickness  $L$  and the bulk at depths larger than  $L$ . All I atoms originating from the surface layer are ejected with a velocity distribution corresponding to a surface temperature  $T_s$ , whereas the I atoms originating from the bulk are assumed to be thermally equilibrated with the surrounding solvent molecules and desorb with the temperature of the bulk liquid  $T_{\text{liq}} = 278$  K.

Profile a in Figure 6 is calculated under the assumption that the IBA molecules in the surface layer of thickness  $L = 1$  nm are oriented with the I end pointing out of the liquid. The translational energy  $E_{\text{trans}}$  of the recoiling fragments I + BA is estimated by a soft impulsive model. According to this model, the initial repulsive force acts only between the I and the attached C atom, channeling  $m(\text{I})/m(\text{C}) \approx 10\%$  of the available energy  $E_{\text{avl}}$  into recoil of the I atom. With  $E_{\text{avl}} = h\nu - D_0(\text{I-BA})$  and a bond dissociation energy  $D_0(\text{I-BA}) = 276$  kJ/mol (at 298 K),<sup>25</sup> this corresponds to an average atomic iodine speed of about 450 m/s or a translational temperature  $T_{\text{trans}} = 1100$  K. Although the soft impulsive model gives a lower bound for

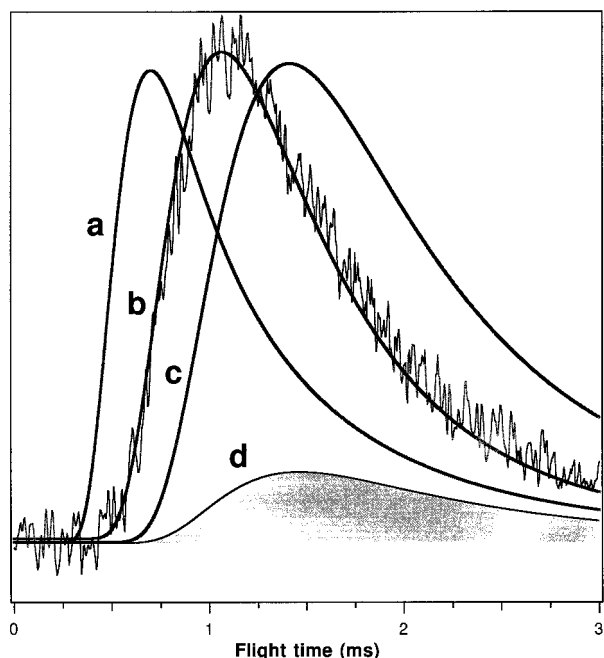


**Figure 6.** Comparison of experimental TOF spectrum of iodine atoms ( $4 \times 10^{-5}$  mol/L IBA in glycerol,  $0.6 \text{ mJ/cm}^2$ ) with model simulations for various temperatures of the surface layer  $T_s$ . A surface layer thickness of 1 nm is assumed. (a)  $T_s = 1100 \text{ K}$ , corresponds to direct ejection of I with energy partitioning according to the soft impulsive model. (b)  $T_s = 480 \text{ K}$  yields the best agreement with the experiment. (c) Isothermal desorption with  $T_s$  equal to the bulk temperature before irradiation,  $T_{\text{liq}} = 278 \text{ K}$ . (d) The contribution to simulation b of I atoms originating from depths greater than 1 nm (multiplied by 10).

$E_{\text{trans}}$ , the calculated TOF distribution displayed in Figure 6a has a too early onset.

The TOF distribution in Figure 6c is obtained with a surface temperature equal to the bulk liquid temperature before irradiation,  $T_s = T_{\text{liq}} = 278 \text{ K}$ . Such a distribution has been found for the  $\text{C}_{18}\text{H}_{37}\text{I/squalane}$  system.<sup>12</sup> The lack of any hyperthermal component was interpreted by a preferential orientation of the chromophores with the iodine end pointing into the liquid. Comparison of the measured spectrum in Figure 6a with the simulation in Figure 6c shows that the experimental profile has an earlier onset than predicted by the isothermal simulation at 278 K.

The best agreement for the IBA/glycerol system was found with a slightly hyperthermal distribution with a temperature for surface layer I atoms  $T_s = 480 \pm 20 \text{ K}$  (Figure 6b). The I atoms from the surface layer are thus ejected before reaching full thermalization with the surrounding liquid. The thickness of the surface layer was varied between 0.1 and 10 nm. Within this range the thickness has only a small effect on the TOF profiles, since even a 0.2 nm surface layer contributes a larger fraction to the total flux than the bulk. The surface layer thickness was fixed at an estimated value of one molecular IBA monolayer of  $L = 1 \text{ nm}$ . The contribution to the best-fit TOF spectrum (Figure 6b) from depths greater than 1 nm is depicted by the dashed area in Figure 6d. Since this diffusive contribution to the total flux is negligibly small compared to the surface layer contribution, the TOF profiles of I atoms from IBA/glycerol can be fitted in a good approximation to a single Maxwell–Boltzmann distribution at  $T = 480 \text{ K}$ .

The cage escape probability  $p_{\text{esc}}$  was varied in the range 0–0.1. For the IBA/glycerol system caging was found to have almost no effect on the shape of the calculated TOF profiles, since  $p_{\text{esc}}$  only affects the desorption yield of those I atoms

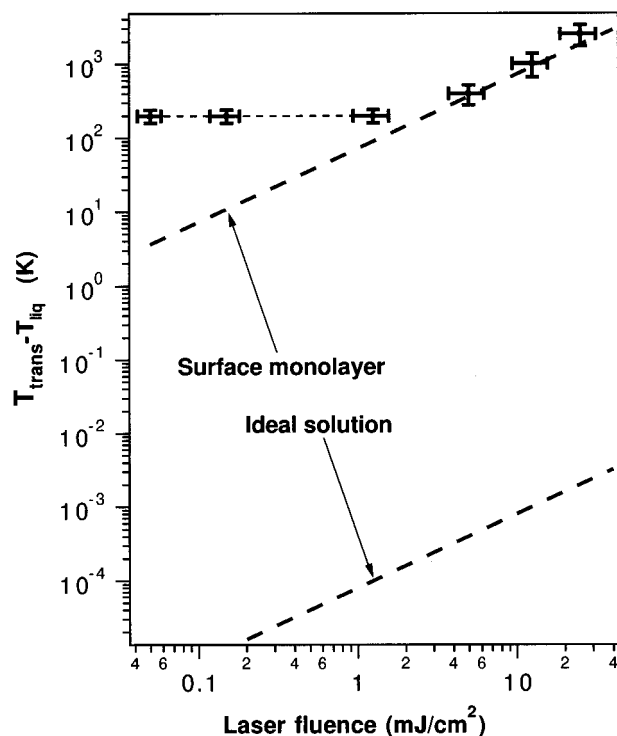


**Figure 7.** Dependence of translational temperature of iodine fragments on the laser fluence. Below  $\sim 5 \text{ mJ/cm}^2$ , a constant temperature of  $480 \pm 30 \text{ K}$  ( $\Delta T = 200 \text{ K}$ ) is found. At higher fluences the temperature rises steeply, indicating explosive desorption. The temperature rise due to laser-induced thermal desorption is calculated for (a) an ideal solution of IBA in glycerol with no surface accumulation of IBA and (b) a surface monolayer of IBA.

originating from depths greater than 1 nm. This contribution to the total I yield is very small because of the low mobility of I atoms in glycerol. However,  $p_{\text{esc}}$  strongly influences the  $\text{I/I}_2$  signal ratio. For  $p_{\text{esc}} = 0$  the yield of  $\text{I}_2$  is zero, since all I fragments from the topmost layer are directly ejected into vacuum and deeper layers give no contribution to the desorption flux. For  $p_{\text{esc}} = 0.1$  the  $\text{I/I}_2$  ratio is 5.8. Good agreement with the experimental value of  $80 \pm 20$  (corrected) is obtained with  $p_{\text{esc}} = 0.005$ .

## 5. Discussion

**Surface Partitioning of IBA.** An aim of this study was to determine the surface concentration of IBA in glycerol using TOF spectroscopy. The TOF results are now compared to the surface tension measurements to elucidate the surface sensitivity of both methods. In an ideal solution the surface concentrations of IBA and glycerol should exactly mirror the concentrations in the bulk liquid. Our TOF results, however, cannot be explained by a homogeneous solution but rather require a surface excess of IBA. The translational temperatures obtained from fits of the TOF distribution (Figure 2) allow an estimate of the density of IBA molecules at the surface. Figure 7 shows the translational temperatures obtained at different laser fluences in the range  $0.05\text{--}20 \text{ mJ/cm}^2$ . The temperature at fluences below about  $5 \text{ mJ/cm}^2$  was found to be constant at  $480 \pm 20 \text{ K}$ . Above  $\sim 10 \text{ mJ/cm}^2$  the temperature rises steeply. The velocity distribution changes from a Maxwell–Boltzmann to shifted Maxwell–Boltzmann distribution with a stream velocity  $v_s$ , indicating explosive desorption. The dashed lines in Figure 7 display the expected translational temperature of I atoms, assuming that the laser energy is immediately converted into heat within the irradiated liquid volume. It is further assumed that the energy

losses by thermal conductivity and photoejection are negligible during the 6 ns irradiation time and that all I atoms desorb with the temperature of the heated liquid. The temperature rise is calculated by

$$\Delta T_s = \Delta T_{\text{liq}} = \frac{hv}{c_v V} \quad (9)$$

where  $hv$  is the fraction of the pulse energy entering the liquid,  $c_v$  is the heat capacity of glycerol (3.0 J/K/cm<sup>3</sup>), and  $V$  is the liquid volume absorbing  $1/e$  of the pulse energy.<sup>26</sup> A reflection loss of 82% of the laser energy due to the grazing incidence angle is taken into account. The lower line corresponds to an ideal solution of IBA in glycerol with no surface accumulation of IBA ( $4 \times 10^{-5}$  mol/L), and the upper line corresponds to a surface fully covered with IBA. The upper line is in good agreement with the experimental data, implying a strong surface excess of IBA in glycerol. The deviations between the upper line and the data points are smaller than the error bounds in laser fluence and temperature.

Similarly, the onset of explosive desorption can be estimated from the product of the absorption cross section of IBA at 275 nm ( $1.5 \times 10^{-17}$  cm<sup>2</sup>), the laser fluence (photons/cm<sup>2</sup>), and the surface concentration of IBA. Explosive desorption occurs when a substantial fraction of a monolayer is desorbed per laser pulse.<sup>22</sup> The collisions of desorbing species in the gas phase result in a shifted Maxwell–Boltzmann velocity distribution, as observed at fluences above  $\sim 10$  mJ/cm<sup>2</sup> (curves c and d of Figure 2). In a perfectly mixed  $4 \times 10^{-5}$  mol/L IBA solution at 10 mJ/cm<sup>2</sup> only a fraction of  $2 \times 10^{-6}$  of a monolayer (ML) desorbs per laser pulse, far too low for explosive desorption. However, with a surface fully covered with IBA (equivalent to a local concentration of 4 mol/L), 0.2 ML is expected to desorb per laser pulse. This fraction is sufficient for ablative desorption, in agreement with the observed onset of shifted Maxwell–Boltzmann velocity distributions.

As noted above, further evidence for a surface excess of IBA was obtained in the dilution study (Figure 3). The reduction of the IBA concentration by a factor of 20 reduces the atomic iodine signal only by a factor of 2–4. A quantitative analysis of the surface accumulation is not attempted at this stage, since the observed concentration dependence may be affected by the film preparation technique (stress-induced fragmentation of the monolayer into islands<sup>20</sup>) as well as limited reproducibility when the liquid sample was exchanged.

In contrast to the TOF data, measurements of the surface tension  $\sigma$  show no evidence of surface partitioning of IBA. At IBA concentrations ranging from  $10^{-6}$  to  $10^{-4}$  mol/L and at temperatures from 5 to 95 °C no deviation of  $\sigma$  was found from the value of pure glycerol, as displayed in Figure 5. The surface tension of water is slightly reduced by IBA (at a concentration near saturation). Since glycerol is less polar than water, it is reasonable to assume that the surface excess free energy  $\Delta G_{\text{excess}}$  (the extra energy the system gains by partitioning IBA to the solution interface) of IBA/water is larger than that of IBA/glycerol. The surface excess of IBA in glycerol is thus expected to be smaller than in water. Compared to  $\sigma$  values of typical surface-active species, which are a factor of  $\sim 3$  lower than  $\sigma$  of pure water, an IBA monolayer probably has a surface tension similar to that of pure glycerol. Therefore, the effect of adding  $10^{-4}$  mol/L IBA to glycerol may be below the detection limits of  $\pm 0.2$  mN/m of our measurement. It is concluded that tensiometry is a rather insensitive technique for detecting low concentrations of dissolved species that are not strongly surface-active. It is particularly insensitive if the surface tensions of

the components are not sufficiently different. The TOF/QMS method, in contrast, is highly sensitive to chromophoric species in the surface layer. This is partly due to an efficient discrimination of the bulk contribution by caging and slow diffusion. A similar difference in sensitivity was found in a comparison of surface excess data from sum-frequency mixing and surface tension measurements.<sup>7</sup>

**Surface Orientation of IBA.** According to the model calculation shown in Figure 6, the velocity distribution of the ejected I atoms can be described by a Maxwell–Boltzmann distribution with a translational temperature  $T_{\text{trans}} \approx 500$  K, 200 K above the temperature of the surrounding liquid and 600 K colder than expected for direct ejection of I from the topmost layer according to a soft impulsive model. The constant value  $T_{\text{trans}} \approx 500$  K found for laser fluences less than or equal to 5 mJ/cm<sup>2</sup> deviates from the prediction for laser-induced thermal desorption from an IBA-covered surface (see upper dashed line in Figure 7). The temperature of the desorbate would be expected to rise linearly with laser pulse energy in the case of thermal desorption. The observed constant translational temperature rather implies incomplete thermalization of the I atoms. The soft impulsive model gives a lower bound for the recoil energy  $E_{\text{trans}}$  of the fragments. Since the observed temperature is below this lower bound, I atoms must lose part of their kinetic energy before leaving the surface. This excludes a preferential surface orientation of IBA molecules with the I atom sticking out of the liquid, because such an orientation allows no energy loss. An orientation of the C–I bond parallel to the surface would ensure at least one collision of the I atoms before desorption. Since the efficiency of translational energy transfer is maximized when the masses are matched, the strongest cooling of an I fragment would be achieved by a collision with an I atom bound to a neighboring IBA molecule. An important aspect of surface ordering may be the formation of IBA dimers at the gas–liquid interface. The dimerization of benzoic acid is known to be almost complete in organic solutions<sup>27</sup> and in the solid.<sup>28,29</sup> By dimerization, the IBA molecules lose their amphiphilic character, which diminishes the orientational forces acting on the surface molecules. This may enhance the preference for surface accumulation of the apolar dimers. Furthermore, dimerization could modify the nature of the electronically excited state and thereby open new channels for loss of translational energy. Corrugation of the surface could also play an important role in translational energy loss, if the gas–liquid interfacial width is similar to or larger than the molecular dimensions. TOF measurements at different temperatures are under way to distinguish between the effect of surface roughness and the average orientation of a single molecule at the surface. The orientation could be changed by using benzoic acids substituted with iodine at different ring positions.

In summary, the TOF data presented here are insufficient to determine the orientation of the surface molecules. Only if the fragments have a velocity distribution similar to that in gas-phase photodissociation, indicating that desorption occurs without inelastic collisions, could one infer an orientation of the excited molecules. This situation has been found in some recent photochemical studies of solid films. Polanyi and co-workers investigated the photolysis of HI adsorbed on LiF and NaF substrates at submonolayer coverage.<sup>18</sup> They observed the ejection of H atoms with a kinetic energy distribution strongly reminiscent of the gas-phase distribution and a background of inelastically scattered H atoms. Methyl nitrite and *tert*-butyl nitrite adsorbed on solid substrates have also been studied in detail. The velocity distribution of the photodesorbed NO was

**TABLE 1: Summary of Results from TOF Analysis for the Systems IBA/Glycerol and C<sub>18</sub>H<sub>37</sub>I/Squalane**

	IBA/glycerol	C <sub>18</sub> H <sub>37</sub> I/squalane
photoproducts detected by TOF/QMS	I, I <sub>2</sub>	I, HI, I <sub>2</sub>
product ratio (corrected)	80:1	5:10:1
T <sub>trans</sub> of I atoms (at <10 mJ/cm <sup>2</sup> )	480 K	298 K
cage escape probability	0.5%	2%
origin of 99% of I flux (depth below surface)	<1 nm	~200 nm
concentration dependence of m/e = 127 signal	strongly sublinear	linear

found to depend on the film thickness and the nature of the substrate and varies from gas-phase behavior to much slower velocity distributions.<sup>17,30,31</sup> In contrast to these studies, the nature of the substrate is unimportant in this work, since the liquid film has a thickness of several thousand molecular layers.

## 6. Summary

Compared to solid surfaces, a rather limited number of methods is available for the study of surfaces of *liquids*, despite their importance in many natural reactions. This work reports on an application of TOF/QMS to the study of a liquid surface and its photochemistry in high vacuum. TOF spectra of photofragments ejected from the liquid surface into the gas phase are analyzed using model calculations, which take into account photolysis of the solute, kinetics of the radicals in the liquid, diffusion, and surface evaporation of the volatile photoproducts, and allow for direct ejection of hyperthermal photofragments into the gas phase. Table 1 summarizes the analysis of the TOF results of IBA/glycerol, together with the previously obtained data on C<sub>18</sub>H<sub>37</sub>I/squalane. In both systems the measurements were taken under low-fluence conditions where laser-induced heating is negligible.

The flux of desorbing species after a laser pulse consists of both cases of atomic and molecular iodine, and HI is an additional photoproduct only produced in the alkyl iodide solution. The different yields of the volatile photoproducts reflect differences in the set of bulk radical reactions and the viscosity of the solvent. The cage escape probabilities of 0.5% (I + BA) and 2% (C<sub>18</sub>H<sub>37</sub> + I) are in agreement with the data of Noyes et al.<sup>32</sup> who studied I<sub>2</sub> photolysis in a variety of solvents and found decreasing cage escape with increasing solvent viscosities. Iodine atoms desorbing off IBA/glycerol originate almost entirely from the topmost liquid layer (<1 nm), whereas the TOF spectra of alkyl iodide solutions probe a depth of ~100 nm. The high surface sensitivity of the TOF/QMS method in the IBA/glycerol system is due to efficient caging and the low mobility of photofragments in glycerol.

Velocity distributions obtained from the TOF spectra indicate that the I atoms desorbing from IBA/glycerol are only partially thermalized by collisions with neighboring surface molecules (T<sub>trans</sub> ≈ 480 K), whereas the velocity distribution of I atoms from C<sub>18</sub>H<sub>37</sub>I/squalane can be described by the temperature of the liquid (T<sub>trans</sub> = 298 K). This indicates that the IBA molecules at the liquid surface are oriented in such a way that on average the I fragments undergo only few collisions before leaving the liquid, whereas C<sub>18</sub>H<sub>37</sub>I molecules have a preferential surface

orientation with the I end pointing into the liquid. After a diffusion length of ~10 nm to reach the surface, these I atoms are therefore fully thermalized.

The onset of explosive desorption from IBA/glycerol and the concentration dependence of the TOF signal are interpreted by a surface excess of IBA. The surface excess is not apparent from tensiometric measurements. Further TOF experiments are under way to determine the surface accumulation and orientation of IBA molecules quantitatively. Second harmonic generation or sum frequency mixing are also considered as additional methods for measuring the surface orientation of IBA.

**Acknowledgment.** This work was supported by the Swiss National Foundation. The author thanks Dr. G. E. Hall for his help with the spectral simulations, Dr. R. T. Carter for carefully reading the manuscript, and Professor J. R. Huber for his generous support.

## References and Notes

- (1) Crutzen, P. J.; Arnold, F. *Nature* **1986**, *324*, 651.
- (2) Prather, M. J. *Nature* **1992**, *355*, 534.
- (3) Rodriguez, J. M.; Ko, M. K. W.; Sze, N. D. *Nature* **1991**, *352*, 134.
- (4) Turro, N. J. *Modern molecular photochemistry*; University Science Books: Mill Valley, CA, 1991.
- (5) Shen, Y. R. *Nature* **1989**, *337*, 519.
- (6) Saecker, M. E.; Nathanson, G. M. *J. Chem. Phys.* **1993**, *99*, 7056.
- (7) Baldelli, S.; Schnitzer, C.; Shultz, M. J.; Campbell, D. J. *J. Phys. Chem. B* **1997**, *101*, 4607.
- (8) Baldelli, S.; Schnitzer, C.; Shultz, M. J.; Campbell, D. J. *J. Phys. Chem. B* **1997**, *101*, 10435.
- (9) Radüge, C.; Pflumio, V.; Shen, Y. R. *Chem. Phys. Lett.* **1997**, *274*, 140.
- (10) Zhu, X.-Y. *Annu. Rev. Phys. Chem.* **1994**, *45*, 113 and references therein.
- (11) Furlan, A. *Chem. Phys. Lett.* **1997**, *275*, 239.
- (12) Furlan, A.; Hall, G. E. *J. Chem. Phys.* **1998**, *109*, 10390.
- (13) Lednovich, S. A.; Fenn, J. B. *AIChE J.* **1977**, *23*, 454.
- (14) Dzvonik, M.; Yang, S.; Bersohn, R. *J. Chem. Phys.* **1974**, *61*, 4408.
- (15) Kawasaki, M.; Lee, S. J.; Bersohn, R. *J. Chem. Phys.* **1977**, *66*, 2647.
- (16) Cheng, P. Y.; Zhong, D.; Zewail, A. H. *Chem. Phys. Lett.* **1995**, *237*, 399.
- (17) Simpson, C. J.; Griffiths, P. T.; Towrie, M. *Chem. Phys. Lett.* **1995**, *234*, 203.
- (18) Barclay, V. J.; Hung, W.-H.; Keogh, W. J.; Kühnemuth, R.; Polanyi, J. C.; Jennison, D. R.; Li, Y. S. *J. Chem. Phys.* **1996**, *105*, 5005.
- (19) Felder, P. *Chem. Phys.* **1990**, *143*, 141.
- (20) Gaines, G. L. *Insoluble Monolayers at the Liquid Gas Interface*; Wiley: New York, 1966.
- (21) At high laser fluences (≤5 mJ/cm<sup>2</sup>) a signal also appeared at m/e = 121 (BA), 248 (IBA), and 92 (glycerol).
- (22) Kelly, R. *J. Chem. Phys.* **1990**, *92*, 5047.
- (23) Miller, D. R. In *Atomic and Molecular Beam Methods*; Scoles, G., Ed.; Oxford University Press: Oxford, 1988.
- (24) Atkins, P. W. *Physical Chemistry*; Oxford University Press: Oxford, 1998.
- (25) McMillen, D. F.; Golden, D. M. *Annu. Rev. Phys. Chem.* **1982**, *33*, 493.
- (26) Volume is given by the spot size (0.12 cm<sup>2</sup>) and the 1/e penetration depth  $d = 1/(\epsilon c)$ , where  $\epsilon$  is the extinction coefficient and  $c$  the local IBA concentration.
- (27) Davis, J. C.; Pitzer, K. S. *J. Phys. Chem.* **1960**, *64*, 886.
- (28) Nagaoka, S.; Terao, T.; Imashiro, F.; Saika, A.; Hirota, N.; Hayashi, S. *Chem. Phys. Lett.* **1981**, *80*, 580.
- (29) Neukomm, M. A. *Ber. Bunsen-Ges. Phys. Chem.* **1998**, *102*, 325.
- (30) Fieberg, J. E.; Szulcowski, G. J.; White, J. M. *Chem. Phys. Lett.* **1998**, *290*, 268.
- (31) Jenniskens, H. G.; Philippe, L.; Essenberg, W. v.; Kadodwala, M.; Kleyn, A. W. *J. Chem. Phys.* **1998**, *108*, 1688.
- (32) Booth, D.; Noyes, R. M. *J. Am. Chem. Soc.* **1960**, *82*, 1868.